Polymer Chemistry

ROYAL SOCIETY OF CHEMISTRY

PAPER

View Article Online
View Journal | View Issue

Cite this: *Polym. Chem.*, 2022, **13**, 3815

Grafting density and antifouling properties of poly[*N*-(2-hydroxypropyl) methacrylamide] brushes prepared by "grafting to" and "grafting from"†

Yu-Min Wang, [a,b] Anna Kálosi,[c,d] Yuriy Halahovets,[d] Iryna Romanenko,[a,b] Jiří Slabý, [e] Jiří Homola, [e] Jan Svoboda, [a] Andres de los Santos Pereira *[a] and Ognen Pop-Georgievski *[a]

Antifouling polymer brushes are widely utilized in biomedical applications to prevent non-specific interactions with biological fluids. They consist of surface-tethered polymer chains and are commonly formed when the chains are "grafted to" (GT) a surface by chemisorption or "grafted from" (GF) a surface in a surface-initiated polymerization. Although the antifouling polymer brushes have been studied for years, an accurate comparison between the GT and GF methods in terms of the ability of the prepared brushes to resist fouling has not been established yet. In this study, we investigate physical and antifouling properties of poly[*N*-(2-hydroxypropyl) methacrylamide] (poly(HPMA)) brushes synthesized by GT and GF methods using reversible addition–fragmentation chain-transfer (RAFT) polymerization. Using size exclusion chromatography and single-molecule force spectroscopy, we are able to ensure that grafted polymer chains in the layers prepared by both methods have comparable composition and molar mass. Thus, we attribute the differences in fouling resistance and physical properties of the polymer layers to the physical conformation of the chains achieved by the selected grafting method. While both types of poly(HPMA) brushes are shown to substantially reduce fouling from blood plasma, the GF polymer brushes suppress fouling by an order of magnitude better than the GT polymer brushes. The observed difference in the antifouling performance is related to the much higher grafting density that can be achieved in the GF method. This study highlights the importance of the selection of the grafting method for achieving a high antifouling performance.

Received 14th April 2022,
Accepted 6th June 2022

DOI: 10.1039/d2py00478j

rsc.li/polymers

Introduction

When artificial materials or devices are brought in contact with bodily fluids, such as blood or blood plasma, the deposition of proteins, bacteria, cells, and microorganisms on surfaces (fouling) takes place. This deposition occurs immediately upon contact of the material with the bodily fluids and poses severe challenges for the development of microfluidic devices, artificial implants, biosensors, and drug delivery systems. On blood-contacting indwelling devices, fouling can trigger life-threatening complications including infection, inflammation, platelet adhesion and activation, blood coagulation, and thrombus formation. Therefore, materials that efficiently prevent the non-specific binding from biological media (referred to as "antifouling materials") are urgently needed to enable the development of new medical devices and to improve the performance of the existing ones.[1–4]

Several types of coatings, such as self-assembled monolayers (SAM) with hydrophilic headgroups, have been demonstrated to reduce non-specific adsorption of individual proteins from model solutions.[5–7] However, the suppression of fouling from blood plasma has been shown to be considerably more challenging due to the complexity and high protein content of this fluid.[8] Polymer coatings have been pursued as one of the most effective approaches to combat blood plasma fouling.[9] The polymers that have been most extensively researched for the development of antifouling coatings are

[a]*Institute of Macromolecular Chemistry, Czech Academy of Sciences, Heyrovsky sq. 2, 16206 Prague, Czech Republic. E-mail: santospereira@imc.cas.cz, georgievski@imc.cas.cz*
[b]*Department of Physical and Macromolecular Chemistry, Charles University, Hlavova 8, 12800 Prague, Czech Republic*
[c]*Centre for Advanced Materials Application, Slovak Academy of Sciences, Dúbravská cesta 9, 84511 Bratislava, Slovakia*
[d]*Department of Multilayers and Nanostructures, Institute of Physics, Slovak Academy of Sciences, Dúbravská cesta 9, 84511 Bratislava, Slovakia*
[e]*Institute of Photonics and Electronics, Czech Academy of Sciences, Chaberská 1014/57, 18251 Prague, Czech Republic*
† Electronic supplementary information (ESI) available. See DOI: **https://doi.org/10.1039/d2py00478j**

poly(ethylene glycol) (PEG), zwitterionic polymers, poly(2-oxazoline)s, poly(2-hydroxyethyl methacrylate), and poly[*N*-(2-hydroxypropyl) methacrylamide] (poly(HPMA)).[10–20] There are two main barriers to fouling on polymer coatings, which can be explained from the perspective of the free energy associated with the process: an enthalpic barrier related to the hydration of the polymer layer, and an entropic barrier, originating from the loss of polymer conformational freedom upon protein adsorption. The enthalpic barrier is a consequence of the removal of water molecules from the hydrophilic polymer layer due to the protein adsorption that results in an energy penalty. The entropic barrier is associated with the compression of the polymer chains when the proteins approach, limiting the polymer conformational freedom.[21–27] A high number of polymer chains per area (called "grafting density") and a small distance between two contiguous polymer chains (called "packing distance") force the polymer chains into a stretched regime, which results in the formation of a "polymer brush". Importantly, both barriers to fouling become larger when the brush character of the grafted polymer layer is more pronounced.[28–34] Therefore, grafting hydrophilic polymers into a predominantly stretched brush regime is one of the important prerequisites for the development of efficient antifouling surfaces.

In order to create polymer brushes, polymers are typically immobilized on surfaces using the "grafting to" (GT) or "grafting from" (GF) approaches. Specifically, the GT method consists of tethering the polymer chains synthesized beforehand "to" the surface from melt or a polymer solution. Careful tuning of the GT conditions may provide densely grafted polymer chains in the brush regime.[14,24,35–37] In contrast, in the GF method, the polymer chains grow *in situ* from surface-bound initiating moieties in surface-initiated (SI) polymerization. Controlled radical polymerizations, such as atom transfer radical polymerization (ATRP) and reversible addition–fragmentation chain transfer (RAFT) polymerization are typically used.[38] The two grafting methods are inherently different and thus have different advantages and disadvantages. The GT method is simpler to perform, but as the polymer chains start to attach to the surface, they sterically hinder the attachment of additional polymer chains, thus limiting the mass of polymer that can be grafted and the achievable thickness.[39] The controlled radical polymerizations employed in the GF method can bypass this limitation. The polymer chains grow already on the substrate from surface-bound initiators and in parallel, not hindering each other and making it possible to tune the thickness in a very wide range.[19] Nevertheless, the controlled radical polymerizations are rather time-consuming and the reaction conditions are stringent.

Moreover, assessing the degree of chain stretching in brushes obtained by GF, *i.e.* determining their grafting density, is highly challenging.[22,27] This issue is important, as the optimization of the grafting density strongly influences the antifouling properties of the layer, as observed previously and widely reported for layers prepared by GT.[14,24,35,36] In order to assess the grafting density, one needs to estimate the number of polymer chains per area unit. This is calculated from the polymer mass (based on the thickness of the polymer layer) and the molar mass of the polymer. In the GT method, this is straightforward as the molar mass of polymers can be measured through size exclusion chromatography (SEC) before grafting (although as reported by Barner-Kowollik *et al.* polymer fractionation needs to be considered if the sample is non-monodisperse).[27,40] However, SEC is not suitable for directly measuring the molar mass of the polymer brushes obtained *via* the GF method because of the extremely small mass of polymer that can be recovered from the surface for the measurement, unless very large areas of substrate are coated.[41] Several research groups suggested to overcome this problem by performing the GF method with an additional free initiator or chain transfer agent (CTA) added in solution to simultaneously obtain free polymer for the SEC measurement.[42–44] Nevertheless, this strategy has been shown rather unreliable, as the polymerization kinetics in solution and on the surface may differ significantly. Indeed, it has been reported that the polymers generated from the soluble initiator and from the surface-bound initiating species during GF may exhibit different molar masses.[26,45] Therefore, the molar mass of the surface-grafted polymer needs to be evaluated independently to ensure a reliable estimation of the grafting density when employing the GF method.

The difficulties in assessing the molar mass in GF polymer layers have hindered their accurate comparison with polymer brushes prepared by the GT method. A quantitative evaluation of the effect of the grafting method on antifouling layer performance has so far been elusive, because of the challenge of preparing polymer brushes with chains of comparable chemical composition and molar mass by the two methods.

In this report, we compare poly(HPMA) brushes obtained by the GT and GF methods at equal polymer molar mass to assess the influence of the grafting method on the antifouling characteristics of the coating and show that they correlate with their brush character. We employed atomic force microscopy-based single-molecule force spectroscopy (SMFS) to assess the polymer chains' molar mass, synthesized on the surface *via* the GF method. SMFS was previously introduced to study the molar mass of surface-grafted polymer chains.[27,45–47] Importantly, the molar mass of the polymer used for the GT method (monitored by SEC) was tuned to match the molar mass of the GF-polymer brush. We observed that GF-poly(HPMA) prepared by surface-initiated RAFT polymerization achieved an order of magnitude lower fouling from blood plasma than poly(HPMA) brushes obtained by an optimized GT method at the same molar mass. The results indicate that the superior resistance to fouling of GF-poly(HPMA) brushes, among the highest ever reported, is attributable to their high grafting density, which is three-times higher than that of GT-brushes. This highlights the critical role of the grafting method when designing end-grafted polymer layers with a brush architecture as it determines their antifouling ability.

Experimental section

Materials

Silicon wafers (orientation ⟨100⟩) bearing a native silicon oxide layer were purchased from Siegert Wafer GmbH (Germany). Silicon wafers coated with Au (150 nm) and glass slides for surface plasmon resonance measurements coated with Au (50 nm) or Au (50 nm) and SiO_2 (15 nm) overlayer were obtained from the Institute of Photonics and Electronics, CAS (Czech Republic). Copper(I) bromide (CuBr, 99.99%), 2,2′-bipyridyl (BiPy, 99%), 4-cyano-4-(phenylcarbonothioylthio) pentanoic acid (CTA), triethylamine (TEA, 99.5%) and hexylamine (99%) were purchased from Sigma-Aldrich (Czech Republic). 4,4-Azobis[2-(imidazolin-2-yl) propane] dihydrochloride (VA-044) was purchased from Wako. TEA was purified by distillation over CaH_2 before use. All other reagents were used as received. Dimethyl sulfoxide (DMSO), toluene, and methanol were purchased from Acros Organics (extra dry, kept over molecular sieves, and filtered using a 0.22 μm syringe filter before use). The other organic solvents of analytical grade were from Lach-Ner (Czech Republic) at the highest available purity and used as received. Deionized (DI) water was obtained from a Milli-Q purification system (Milli-Q gradient A10, Merck-Millipore). [11-(2-Bromo-2-methyl)-propionyloxy] undecyltrichlorosilane (Br-silane) and the monomer *N*-(2-hydroxypropyl) methacrylamide (HPMA) were synthesized according to procedures reported earlier.[20,48] Human serum albumin (HSA) and human fibrinogen (Fbg) were purchased from Sigma-Aldrich (Czech Republic). Pooled human blood plasma (HBP, mix of 5 donors) was obtained from the Institute of Hematology and Blood Transfusion (Czech Republic).

Self-assembled monolayer on the substrates and CTA immobilization

First, the silicon substrates were cleaned by rinsing with ethanol and DI water twice, dried under a stream of nitrogen, and then activated in a UV/O_3 cleaner for 20 min. Immediately, they were immersed in a 0.1% v/v solution of Br-silane in anhydrous toluene and kept in a dry environment at room temperature for 3 h. The silicon substrates coated with a self-assembled monolayer of Br-silane (Br-SAM) were then washed with toluene, acetone, and twice with ethanol and DI water, then dried under a stream of nitrogen.[11] Subsequently, the Br-SAM substrates were placed in reactors under argon atmosphere and a solution of CTA (66.69 mg, 0.239 mmol), CuBr (6.10 mg, 42.5 μmol), and BiPy (12.99 mg, 83.2 μmol) in deoxygenated anhydrous DMSO (10 mL), previously purged by argon bubbling 30 min, was added under argon and left to react for 24 h at 30 °C to obtain the CTA-SAM.[49] After the modification, the CTA-SAM substrates were washed with methanol, acetone, and twice with ethanol and DI water, then dried under a stream of nitrogen.

RAFT polymerization of HPMA for GT and GF polymer layers

The polymerization of HPMA *via* RAFT was performed by the same procedure to obtain poly(HPMA) in solution for subsequent GT method or on CTA-SAM substrates to obtain GF-poly(HPMA) brushes directly.[50] A flask containing HPMA (500 mg, 3.49 mmol), CTA (1.3 mg, 4.65 μmol), and VA-044 (0.75 mg, 2.33 μmol) sealed with a septum was purged with argon for 1 h in an ice bath. Anhydrous methanol was purged with argon in parallel for 1 h and 2 mL were transferred to the flask containing the solids. The resulting mixture was stirred until full dissolution. For the SI-RAFT used in the GF method, the polymerization solution was added under argon protection to individual reactors containing CTA-SAM-coated silicon substrates or SiO_2-coated chips for surface plasmon resonance (SPR), previously sealed and deoxygenated by three pump-refill cycles with argon. RAFT polymerization was carried out by placing the flask containing the reaction mixture or the reactors containing the substrates in the reaction mixture in a temperature-controlled oil bath at 45 °C for a set time between 1.5 hours and 25 hours. The polymerization was quenched by opening the reaction vessels to the atmosphere and rapidly cooling the solution in an ice bath. To isolate poly(HPMA), the solution was dialyzed (membrane molecular weight cut-off 1000 Da) against DI water, which was regularly renewed for 24 hours, and then lyophilized. Substrates coated with the GF-poly(HPMA) brushes were rinsed with methanol, acetone and twice washed by ethanol and DI water, then dried under a stream of nitrogen.

Aminolysis of poly(HPMA) with CTA end groups

Both poly(HPMA) recovered from solution and GF-poly(HPMA) brushes were terminated with thiocarbonylthio (S–C═S) end groups after RAFT polymerization. The CTA groups of poly (HPMA) used for GT and of the GF-poly(HPMA) brushes prepared for SMFS measurements were converted to thiol (–SH) *via* aminolysis following a modified literature procedure.[47] A flask of anhydrous ethanol and a flask containing hexylamine (20 μL, 0.153 mmol) and TEA (20 μL, 0.143 mmol) were deoxygenated by purging with argon for 10 min. The reaction solution was prepared by adding 5 mL of degassed ethanol into the flask with the amines. To aminolyze the poly(HPMA)-CTA collected from solution, 5 mL of the reaction solution was added under argon to a flask containing 25 mg of the polymer, previously deoxygenated, and the reaction was allowed to proceed at room temperature for 3 h. The poly(HPMA) with thiol moiety (poly(HPMA)-SH) was recovered after dialysis and lyophilization. For GF-poly(HPMA) brushes, the aminolysis process was the same, but the substrates coated with poly (HPMA) brushes were placed in reactors instead of polymer collected from solution. Afterwards, the substrates coated with poly(HPMA)-SH brushes were washed with methanol, acetone, and twice with ethanol and DI water, then dried under a stream of nitrogen.

Poly(HPMA)-SH grafted to the surfaces under good solvent and poor solvent conditions

First, the bare gold wafer substrates or SPR chips were cleaned by rinsing with ethanol and DI water twice, dried under a stream of nitrogen, and then activated in a UV/O_3 cleaner for

20 min. In parallel, a polymer solution of poly(HPMA)-SH was prepared at 1 mg mL^{-1} in DI water (transparent solution) as a good solvent condition or in 0.75 M $Na_2SO_{4(aq)}$ for cloud point achievement as a poor solvent condition. Then, the freshly cleaned gold wafer substrates or SPR chips were placed immediately in reactors followed by adding a solution of poly(HPMA)-SH under good solvent condition or poor solvent condition for 20 h at 28 °C under argon atmosphere for the binding between thiol and gold to occur. The GT-poly(HPMA) surfaces were rinsed with DI water, acetone and twice washed by ethanol and DI water, then dried with a stream of nitrogen.

X-ray photoelectron spectroscopy (XPS)

Measurements were performed using a K-Alpha$^+$ XPS spectrometer (ThermoFisher Scientific, UK) operating at a base pressure of 1.0×10^{-7} Pa. The data acquisition and processing were performed using the Thermo Avantage software. To limit the X-ray induced destruction of the thin polymer films and maximize the signal-to-noise ratio, individual points were measured within areas covering 8 × 8 mm^2. At each point, high-energy resolution core level spectrum was measured using a microfocused, monochromated Al Kα X-ray radiation (spot size of 400 μm, pass energy of 150 and 50 eV for survey and high-resolution measurements, respectively). All reported XPS spectra are averages of 24 individual measurements. The spectra were referenced to the C 1s peak of hydrocarbons at a binding energy of 285.0 eV controlled using photoelectron peaks of PET and metallic Cu, Ag, and Au standards. The atomic concentrations of the different chemical moieties were determined from the respective photoelectron peak areas of levels Br 3d, Au 4f, Si 2p, S 2p, C 1s, N 1s, and O 1s high-resolution spectra after modifying Shirley's inelastic background subtraction. Assuming a simple model of a semi-infinite solid of homogeneous composition, the peak areas were corrected for the photoelectric cross-sections, the inelastic mean free paths of the electrons in question, and the transmission function of the spectrometer used.[51] All spectra with high resolution were fitted using Voigt profiles. The experimental uncertainties in the quantitative analysis of XPS were assessed to be below 10%. The value covers the overall uncertainties due to variations connected to sample preparation and the XPS background subtraction.

Spectroscopic ellipsometry (SE)

Ellipsometric data were acquired using a J.A. Woollam M-2000X spectroscopic ellipsometer operating in rotating compensator mode at angle of incidence (AOI) range 60–71° (with a step of 1°) and spectral range of λ = 250–1000 nm. See ESI† for detailed information on the used setup for *in situ* measurements and SE data analysis.

SEC-multiple angle laser light scattering (SEC-MALLS)

The poly(HPMA) synthesized by RAFT polymerization for GT, poly(HPMA) collected in solution during GF, and poly(HPMA)-SH by aminolysis were measured by using a Shimadzu HPLC system equipped with a Superose 12 column, online UV detector (Shimadzu), differential refractive index detector (Wyatt Optilab T-rEX) and multi-angle light scattering (Wyatt Dawn Heleos-II). The mobile phase used for the measurement was 0.3 M sodium acetate buffer (pH 6.5) with 1 g L^{-1} of sodium azide flowing at 0.5 mL min^{-1}, and the specific refractive index increment dn/dc of poly(HPMA) was applied as 0.167.

AFM-based single molecule force spectroscopy (SMFS)

Topographical AFM micrographs were obtained on a Bruker MultiMode 8 microscope using silicon nitride triangular-shaped cantilevers with a nominal spring constant of 0.4 N m^{-1} and tip radius of 2 nm. Areas of 2 × 2 μm^2 and 500 × 500 nm^2 were scanned by 512 × 512 points each. The obtained images were analyzed in Gwyddion software. SMFS measurements were performed using the same AFM microscope working in contact mode in a fluid cell with gold-coated tips (MikroMasch, HQ:CSC38/Cr–Au, consisting of three cantilevers with a nominal tip radius of 35 nm). The SMFS measurements were carried out in DI water. After mounting the cantilever, sensitivity, and spring constant measurements were performed prior to the SMFS measurements. Thousands of force curves were measured for each sample distributed across the sample surface. The tip separation from the sample was 300 nm, and the movement was performed with a frequency of 0.5 Hz. The data were firstly processed by in-house developed software (written in LabVIEW), where the curves showing a clear unfolding and rupture event were selected. In the case of the poly(HPMA)-SH on silicon substrate samples, 4% of the recorded curves showed a rupture event. These curves were further fitted to the worm-like chain (WLC) model to obtain the contour and persistence length of the GF-poly(HPMA) brushes and thus probe their corresponding molar mass.[47,52] See ESI† for further information on AFM topographical micrographs and SMFS data analysis.

Calculation of surface parameters of grafted poly(HPMA) layers

The density $\sigma = \frac{h\rho N_A}{M_n}$ and the distance between grafting sites supposing hexagonal packing $D = \sqrt{\frac{2}{\sqrt{3}\sigma}}$ were estimated utilizing the layer thickness in the dry state as determined by ellipsometry (h), the bulk density of poly(HPMA) ρ was taken to be 1.1 g cm^{-3}, and N_A is the Avogadro constant. The radius of gyration R_g for poly(HPMA) M_n 49.0 kg mol^{-1} in water was calculated to be 7.4 nm.[53] The overlap parameter $\frac{D}{2R_g}$ can be utilized to describe the state of tethered polymer chains. Values of (i) $\frac{D}{2R_g} > 1.0$ indicate that the polymer chains are in a "mushroom" state; (ii) $\frac{D}{2R_g}$ close to 1.0 are characteristic for a mushroom-to-brush transition; whereas (iii) $\frac{D}{2R_g} < 0.5$ are indicative that the chains stretch away from the surface and attain brush conformation.[54,55]

Surface plasmon resonance (SPR)

Non-specific protein adsorption on the bare SPR chip, SiO_2-coated SPR chip, poly(HPMA) grafted-from SiO_2-coated SPR chip, and poly(HPMA) grafted-to SPR chip was measured using an SPR instrument based on the Kretschmann geometry of the attenuated total reflection and spectral interrogation. In this system, the shift in the resonance wavelength was recorded, and the amount of the biomolecules adsorbed on the coating was estimated from the difference between the baselines in pure PBS (pH 7.4) before and after contact with the tested solutions: HSA (5 mg mL^{-1} in PBS), Fbg (1 mg mL^{-1} in PBS) and HBP (undiluted). The solutions were pushed through a 4-channel flow cell attached to an SPR chip for 15 min. The measurements were performed at a flow rate of 25 μL min^{-1} and a temperature of 25 °C (±0.1 °C). The fouling (adsorbed mass) was obtained using the calibration of the sensor response described in the next subsection.

Calculation of SPR sensor sensitivity

The sensitivity of SPR measurements depends on the thickness and the refractive index of the polymer overlayer and the resonance wavelength. For this reason, the sensor responses have been calibrated for each chip separately using a theoretical model. First, reflectivity calculations were performed using transfer-matrix method implemented in the EWA toolbox in Matlab.[56] The considered geometry is composed of the semi-infinite dielectric layer (glass, refractive index: 1.51), a metal layer (gold, thickness: 48 nm, refractive index: interpolated from experimental data), dielectric layers (SiO_2, thickness 15 nm, refractive index: 1.49; poly(HPMA) polymer, thickness and refractive index: interpolated from ellipsometric data, Table 1 and Table S1, ESI†), dielectric overlayer (biomolecular layer; only for the sensitivity calculation, thickness: 7 nm; refractive index: 1.40) and a semi-infinite dielectric layer (a buffer; refractive index: 1.33). Second, the sensitivity was calculated from the reflectivity obtained with and without the dielectric overlayer. Sensitivity correction factors of 1.28, 1.10, 1.16, and 1.68 have been obtained and utilized to recalibrate the sensor response of SiO_2-coated SPR chips, GS and PS poly(HPMA) grafted-to SPR chips, and poly(HPMA) grafted-from SiO_2-coated SPR chips, respectively. In order to translate the surface refractive-index change to the surface mass density, an experimental factor of 18 ng cm^{-2} nm^{-1} was used (valid at the wavelength of 750 nm).

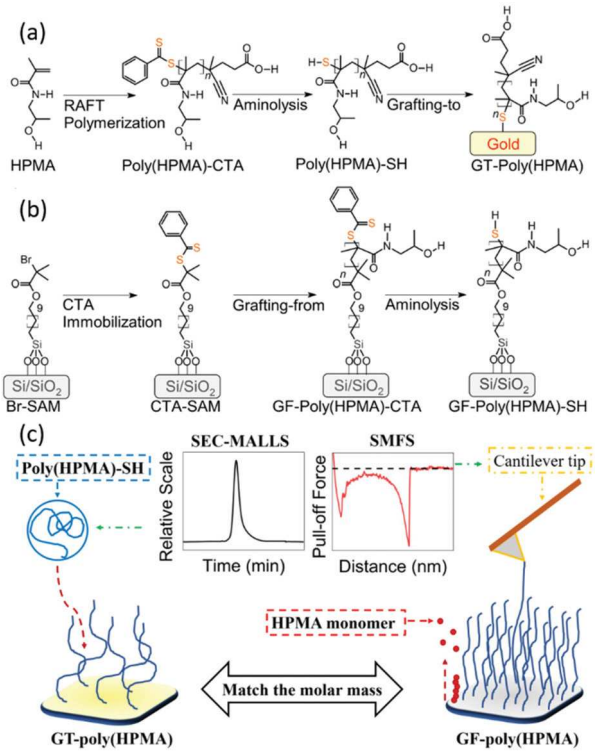

Scheme 1 Synthesis of poly(HPMA) brushes by (a) GT method and (b) GF method. (c) Comparison between GT and GF methods and respective molar mass characterization by SEC-MALLS and SMFS. Note: GF-poly(HPMA)-SH was employed only for SMFS measurements while swelling and fouling experiments were performed on GF-poly(HPMA)-CTA.

Results and discussion

To assess the influence of the different grafting methods on the antifouling properties of poly(HPMA) brushes, we prepared both types of poly(HPMA) coatings with polymer chains of the same molar mass using (SI)-RAFT polymerization (Scheme 1a and b). In this study, GF-poly(HPMA) brushes were directly synthesized on SiO_2-coated substrates, while GT-brushes were prepared by binding poly(HPMA) prepared by solution polymerization onto gold-coated substrates. To match the molar mass of poly(HPMA) grown from the surfaces with the one obtained in solution, these were monitored by means of SMFS and SEC-MALLS, respectively (Scheme 1c). In this way, we can fully characterize the polymer brushes prepared by both grafting methods and directly compare the physical and antifouling properties that they yield.

Table 1 Polymer surface parameters of grafted poly(HPMA) layers by different grafting methods

Poly(HPMA)	M_n [a,b] (kg mol^{-1})	h_{dry} (nm)	σ (chain per nm^2)	D (nm)	$D/2R_g$	$h_{swollen}$ (nm)	Swelling ratio
GT-GS	49.0[a]	2.0 ± 0.1	0.02	7.2	0.49	13.2 ± 0.4	6.5 ± 0.3
GT-PS	49.0[a]	4.1 ± 0.4	0.05	5.0	0.34	18.1 ± 2.1	4.4 ± 0.4
GF	49.0[b]	13.5 ± 0.2	0.18	2.6	0.18	27.2 ± 0.3	2.1 ± 0.1

[a] Number-average molar mass was measured by SEC-MALLS. [b] Number-average molar mass was calculated from the contour length obtained by SMFS.

Poly(HPMA) brushes prepared by "grafting-from": synthesis and molar mass

The GF-poly(HPMA) brushes were prepared by growing the polymer chains in SI-RAFT polymerization directly from surface-bound chain transfer agent on a self-assembled monolayer (CTA-SAM) (Scheme 1b). This CTA-SAM was obtained by modification of a bromine-functional SAM (typically used as initiator in ATRP) in a simple one-step reaction following a protocol based on atom transfer radical addition mechanism.[49] The success of the CTA immobilization was confirmed *via* XPS (Fig. S5, see ESI†). The conditions for this polymerization were optimized based on previous reports for the RAFT polymerization of HPMA in solution.[50,57] Due to the mechanism of SI-RAFT polymerization, the poly(HPMA) grows concurrently in solution from soluble CTA and radical initiator as well as from the surface. The polymerization kinetics were monitored by measurements of the thickness of the polymer layer (*via* spectroscopic ellipsometry in the dry state) and of the molar mass of the polymer in solution (*via* SEC-MALLS). The thickness of the polymer layer increased with increasing polymerization time, reaching 13.5 ± 0.2 nm at 24 h (Fig. 1a). The molar mass of the polymer formed in solution grew with increasing polymerization time, between 4.8 and 47.0 kg mol^{-1} from 1.5 h up to 24 h, while the $Đ$ remained low (Fig. 1b).

In the current study, we selected a thickness of 13.5 nm for GF-poly(HPMA) brushes at an SI-RAFT polymerization time of 24 h. Previous studies of the antifouling properties of similar brushes indicated that a layer thickness above 10 nm provides satisfactory fouling resistance.[11,58–60] At the same time, a thicker brush is associated with a larger molar mass of the grafted polymer.[47] We, therefore, did not further increase the thickness to avoid possible limitations associated with performing GT with very high molar mass polymers.[61]

To accurately measure the molar mass of GF-poly(HPMA) grown from the surface, we employed SMFS, particularly the variant based on an AFM setup. In this technique, individual poly(HPMA) chains bind to the tip of an AFM from their end group and the elastic force required to stretch the chain is recorded as a function of the distance to the surface until the tip–polymer contact ruptures. The obtained curve can be fitted to the worm-like chain (WLC) model to obtain the contour length of polymer chains (see ESI, Fig. S3†), which is used to obtain the number-average molar mass M_n (see ESI, Fig. S4†).[52]

The CTA end groups in the as-prepared poly(HPMA) brushes were converted to thiol (poly(HPMA)-SH) by aminolysis before SMFS measurements in order to maximize binding with the gold-coated AFM cantilever tip (see ESI, Fig. S6†). The GF polymer brushes employed for other measurements were CTA-capped (not aminolyzed) to avoid the possibility of disulphide formation, which would create polymer loops and alter the layer architecture.

The direct measurement of the molar mass of the polymer grown on the surface is necessary to ensure that the comparison between polymer layers formed by GF and GT is valid. The GF-poly(HPMA) brushes of 13.5 ± 0.2 nm thickness presented a number-average contour length (l_c) of 67.2 ± 0.9 nm (Fig. 2 and S3, ESI†). This corresponds to a number-average molar mass of $M_{n,\ GF\text{-}24\ h}$ = 49.0 kg mol^{-1} with a $Đ$ of 1.14 (see ESI, Fig. S4†). The molar mass of poly(HPMA) collected in solution at the same polymerization time was $M_{n,\ solution,\ 24\ h}$ = 44.6 kg mol^{-1} with a $Đ$ of 1.38. Thus, the discrepancy of molar mass between the polymer formed on the surface and in the solution is only slight at approximately 10%. Nevertheless, it is important to note that other studies have found that the polymerization kinetics may vary substantially between surface and solution, leading to much more significant discrepancies in molar mass. These were attributed to mass transport limitations and the crowded environment at the interface. We hypothesize that the slow polymerization kinetics of HPMA under the selected conditions and concomitant long polymerization time to reach the targeted thickness may have partly negated the limiting effect of diffusion that was previously reported for other GF polymerizations.[26]

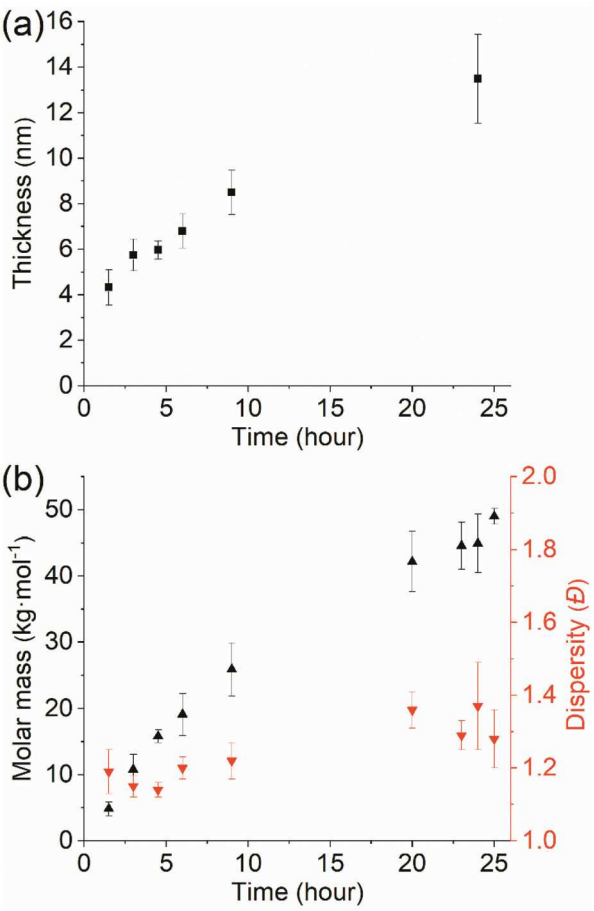

Fig. 1 Kinetic plots: (a) thickness of GF-poly(HPMA) brushes in the dry state measured by SE. (b) Molar mass and $Đ$ of poly(HPMA) generated in the solution of (SI)-RAFT polymerization measured by SEC-MALLS.

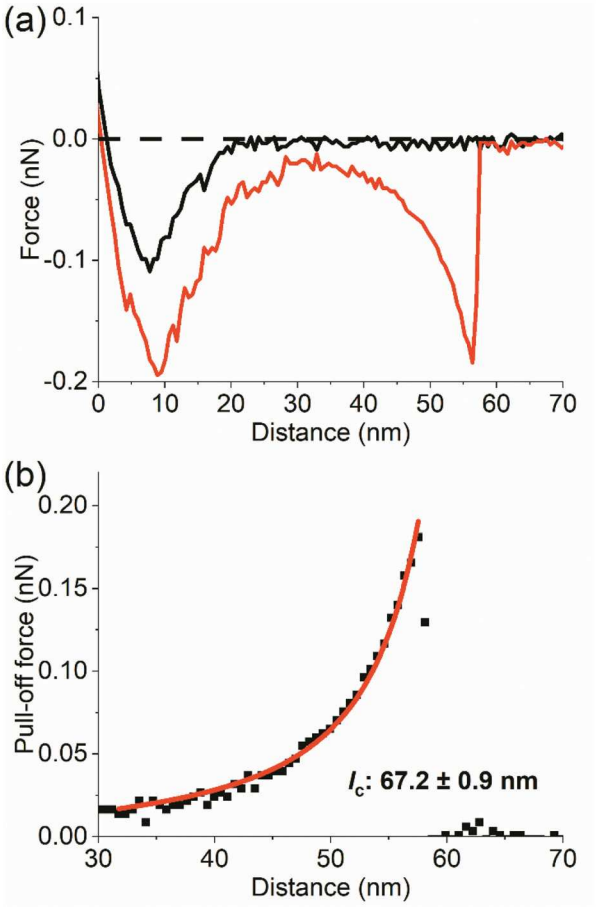

Fig. 2 (a) Representative force–distance curve of selected clear unfolding and rupture event during approach (black) and retraction (red). (b) Characteristic pull-off force curve (black square symbol) with the fitting of WLC model (red line).

Poly(HPMA) brushes prepared by "grafting-to": synthesis and molar mass

The poly(HPMA) synthesized for GT method was prepared by RAFT polymerization and characterized by NMR to confirm the success of the polymerization (see ESI†). We targeted a molar mass for the GT-poly(HPMA) brushes that matched as closely as possible the one of the GF-brushes ($M_{n,\ GF}$ = 49.0 kg mol^{-1}). For this purpose, we slightly extended the RAFT polymerization time compared to the conditions employed to obtain the GF-poly(HPMA) brushes and collected the poly(HPMA) formed in solution at 25 h for use in the GT. This polymer was analyzed by SEC-MALLS, yielding a molar mass of $M_{n,\ GT}$ = 49.0 kg mol^{-1} with a $Đ$ of 1.18 (see ESI, Fig. S8†). Prior to the grafting-to procedure, the CTA end groups of the obtained polymer were aminolyzed to thiols, as these bind strongly to gold surfaces and provide a stable attachment for the GT-poly(HPMA) brushes. The aminolysis reaction did not cause any unwanted changes in the molar mass and chemical structure, as confirmed *via* SEC-MALLS and NMR (see ESI, Fig. S8 and S9†).

Poly(HPMA)-SH was grafted to gold surfaces under two sets of conditions, which differed by the thermodynamic quality of the solvent with respect to poly(HPMA): "good solvent" (GS) and "poor solvent" (PS). In the GS conditions, the gold surfaces were immersed for 20 h in a poly(HPMA)-SH solution in deionized water at 1 mg mL^{-1}. This method is simple to perform and may be considered a reference for comparison with other polymer brush coatings. In contrast, grafting under PS conditions is expected to lead to a smaller packing distance and higher grafting density, as the polymer chains shrink and adopt a more compact conformation, enabling them to pack more densely on the surface during the grafting process due to decreased steric hindrance. To achieve PS conditions, the solvent quality was adjusted by adding Na_2SO_4 and increasing the temperature until the appearance of turbidity to reach the so-called "cloud point". Similar PS conditions were often reported for PEG but rarely applied to other polymers.[24,35] In previous reports, grafting of PEG under PS conditions led to a higher grafting density associated with enhanced fouling resistance. Thus, PS-grafted poly(HPMA) brushes are expected to display higher grafting density and superior antifouling performance in comparison to GS grafting. The key question that needs to be addressed is how these compare to the properties of chemically comparable brushes obtained *via* GF. By comparing these two grafting systems with grafted chains of the same molar mass, we gain understanding about the impact of the grafting method on fouling resistance and surface physical parameters.

Physicochemical characterization of poly(HPMA) brushes prepared by GT and GF methods

The chemical characterization of the grafted poly(HPMA) layers was performed by means of X-ray photoelectron spectroscopy (XPS). In the high-resolution XPS spectra of the C 1s region, all three types of poly(HPMA) brush coatings present identical features of C–C and C–H (285.0 eV), C–C═O (285.4 eV), C–N (286.1 eV), C–O (286.4 eV) and N–C═O (288.1 eV) as shown in Fig. 3 and Table S2 (see ESI†). For the poly(HPMA) bushes performed *via* the GF method, the XPS measurements also detected the presence of CTA end groups. The decrease in sulphur content upon the aminolysis reaction prior to SMFS measurements indicates successful removal of CTA and thiol remaining as the polymer end group (see ESI, Fig. S6†). Moreover, the overall composition of poly(HPMA) was preserved, indicating that the aminolysis did not produce any unwanted changes to the polymer layer intended for SMFS analysis. Besides the previously mentioned observations for GT-poly(HPMA) brushes in the C 1s region, high-resolution XPS spectra of S 2p region further verified the covalent attachment of the thiol end groups to the gold substrate. Namely, after the GT anchoring reaction, we observed shifts in the binding energies from the characteristic free C–S–H thiol contribution at 163.4 eV to C–S–Au thiolate at 161.9 eV (see ESI, Fig. S7†).[62] Fourier-transform infrared spectroscopy (FTIR) further confirmed the successful attainment of the targeted chemical modifications (see ESI, Fig. S10 and S11†).

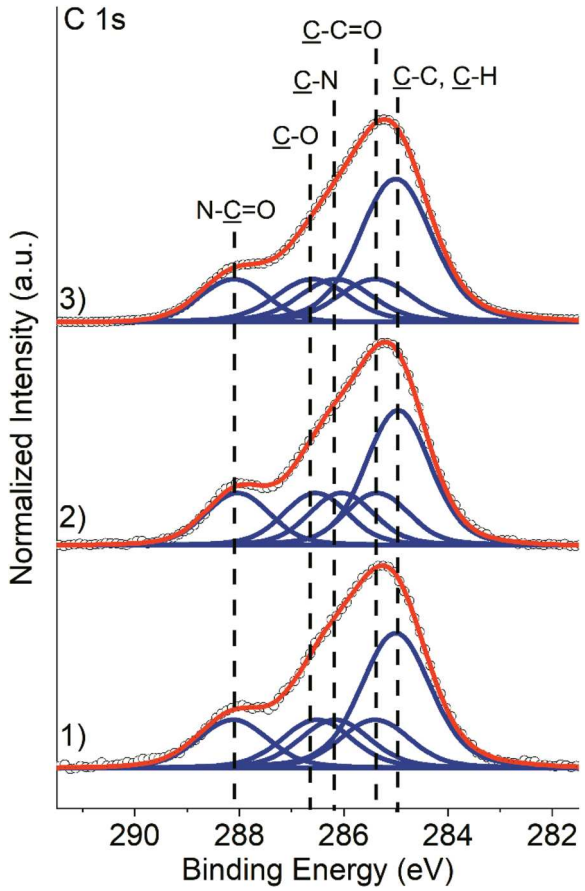

Fig. 3 XPS characterization of each grafted poly(HPMA) layer. High-resolution XPS spectra of C 1s region for the GT-GS-poly(HPMA) on gold substrates (1), GT-PS-poly(HPMA) on gold substrates (2), and GF-poly(HPMA) on silicon substrates (3). Note: Measured high-resolution C 1s spectra are presented with open circles, while their corresponding fitted envelopes are presented with red lines. The individual contributions of different functional groups are represented with blue lines.

Thickness and swelling ratio of poly(HPMA) coatings prepared by GT and GF methods

The thickness of the GT- and GF-poly(HPMA) brushes was measured by spectroscopic ellipsometry, both in the dry state h_{dry} and immersed in water $h_{swollen}$ (Table 1). As the molar mass of poly(HPMA) in the three types of brushes is the same, a thicker layer implies a larger number of polymer chains per unit of area, *i.e.*, higher grafting density.

GT-GS-poly(HPMA) had a dry thickness of 2.0 ± 0.1 nm corresponding to 0.02 polymer chains per nm^2 and a distance between grafting points D of 7.2 nm. This distance is smaller than the dimensions of the polymer coil in solution (given by twice the radius of gyration $2R_g$), which indicates that the chains are slightly stretched in this layer. In contrast, GT-PS-poly(HPMA) presented a larger thickness in the dry state (4.1 ± 0.4 nm), with a correspondingly higher grafting density and a more stretched conformation of the chains, *i.e.*, a more pronounced brush character. Clearly, the poly(HPMA) chains packed more closely together in GT due to the addition of salt and increased temperature. This can be explained by the collapse of the poly(HPMA) conformation under PS conditions, which reduces steric hindrance for their approach to the surface during grafting, analogously as previously reported for PEG.[24] For both types of GT layers, in spite of the absolute grafting density being relatively low, the polymer chains were in the brush regime ($D/2R_g < 0.5$). This is because of a large R_g and polymer chain footprint, resulting from the high polymer molar mass.[24,39] The thickness of GF-poly(HPMA) brushes in the dry state amounted to 13.5 ± 0.2 nm, while their grafting density was 0.18 chains per nm^2, over three times higher than the GT-PS brush. The closer packing in the GF-layer in comparison to even the optimized GT method is possible because of the fundamentally different mechanism by which the polymer brushes are formed in the GF process. While in GT the fully formed polymer chains need to diffuse to the surface so that their end groups can react with the substrate, in GF it is the monomer that needs to reach the surface and add to the polymerization growing centres. Its diffusion is much faster due to their small size and high concentration.

The antifouling properties of the polymer brush layers are relevant in an aqueous solution, with the hydrophilicity of the layers being critical for this effect. We, therefore, measured the water uptake of the poly(HPMA) brushes using *in situ* ellipsometry. The swelling ratio ($h_{swollen}/h_{dry}$) is determined by the energy balance between contributions from enthalpic gain from favourable water–polymer interactions and the entropic penalty from an increasingly stretched polymer conformation.[55,63–67] Interestingly, the swelling ratio in water ranges from 6.5 for GT-GS and 4.4 for GT-PS down to 2.1 for GF-poly(HPMA) brushes, even though all layers consist of chemically similar chains of the same molar mass. This tendency arises from the difference in grafting density yielded by the different grafting methods. For the denser GF brushes, the grafting sites are closer to each other and the polymer conformation is more stretched even in the dry state. In contrast, the polymer chains in the GT-layers are able to swell more when in contact with water as they are less stretched in the dry state. Their higher swelling ratio is also accompanied by a lower refractive index in the swollen state (closer to that of water), indicating a lower polymer volume fraction in swollen layers.[67–69] Thus, the physical characterization of the poly(HPMA) layers prepared by GF, GT-GS and GT-PS proves the dramatic influence of the grafting method in determining the behaviour of the surface-bound polymer chains in an aqueous solution.

Fouling resistance of poly(HPMA) coatings obtained by GT and GF methods

Polymer brushes are of great interest for biomedical applications due to their ability to resist the adsorption of proteins. Previous studies have related this property to the polymer grafting density and chain length, on the basis of theoretical predictions[30,61] and experimental results with PEG coatings prepared *via* GT.[24,28,29,31,33,35,36,70] Nevertheless, the factors behind the fouling resistance of GF-polymer brushes and accu-

rate comparison with GT-layers have so far been elusive due to the difficulties in characterizing the grafting density of GF-polymer coatings and in preparing GT- and GF-coatings with polymer chains of comparable chemical structure and molar mass. We surveyed the antifouling performance of poly(HPMA) coatings prepared by GT and GF using surface plasmon resonance (SPR) to determine the mass of protein adsorbed from various single-protein solutions and blood plasma. The combination of SI-RAFT polymerization with characterization simultaneously by SEC-MALLS and SMFS allowed us to compare GT- and GF-poly(HPMA) brushes in terms of their fouling resistance while keeping the molar mass equal. This highlights the effect of the selected grafting methods on the antifouling properties.

We measured the adsorption from solutions of human serum albumin (HSA, 5 mg mL^{-1}), human fibrinogen (Fbg, 1 mg mL^{-1}), and undiluted human blood plasma (HBP, pooled from 5 donors) by SPR. This technique relies on detecting the change of the refractive index in the immediate vicinity of a bare or coated sensor surface, which accompanies the deposition of proteins. The sensitivity of SPR is affected by the presence of a SiO_2 and/or polymer layer, as the protein adsorption occurs farther away from the SPR-sensor gold surface. In order to correctly compare the fouling on the poly(HPMA) coatings of various thicknesses and the bare gold and SiO_2 sensor surfaces, we modelled the changes in sensitivity for each type of coating and applied the resulting corrections to obtain the actual value of adsorbed protein mass on the surface.

Both HSA and Fbg solutions rapidly fouled the bare gold SPR chips (Fig. 4a and b). SiO_2-coated SPR chips showed slightly smaller adsorption of single proteins than gold, probably due to the strong hydrophilic character of SiO_2 when freshly cleaned, as well as negative charge (isoelectric points of 4.9, 5.8 and 3.9 for HSA, Fbg and SiO_2, respectively).[71,72] Remarkably, poly(HPMA) brushes prepared by the GT-GS method reduced fouling from HSA and Fbg by 89 and 93% in comparison with bare gold, respectively, even though they were only 2 nm-thin in the dry state. The brushes prepared in GT-PS conditions achieved a similar performance as GT-GS brushes for individual proteins (reductions of 86 and 95% for HSA and Fbg, respectively). Nevertheless, it is not possible to clearly rank the antifouling performance of these surfaces against single-protein solutions, as the differences fall within the error of the measurements. The incomplete prevention of fouling from Fbg and HSA by both types of GT layers may be attributed to the small size of the proteins, which is comparable to the packing distance of the polymer chains on both surfaces and may allow penetration into the layer.[39]

In the case of HBP, the most challenging fluid due to its high protein concentration and complexity of composition, both bare gold and SiO_2 displayed very high fouling, on the level of a protein monolayer. The hydrophilicity of SiO_2 was not sufficient even to reduce the fouling from HBP in comparison with gold. In contrast, GT-GS- and GT-PS-brushes suppressed fouling by 81 and 89%, respectively. The over two-fold

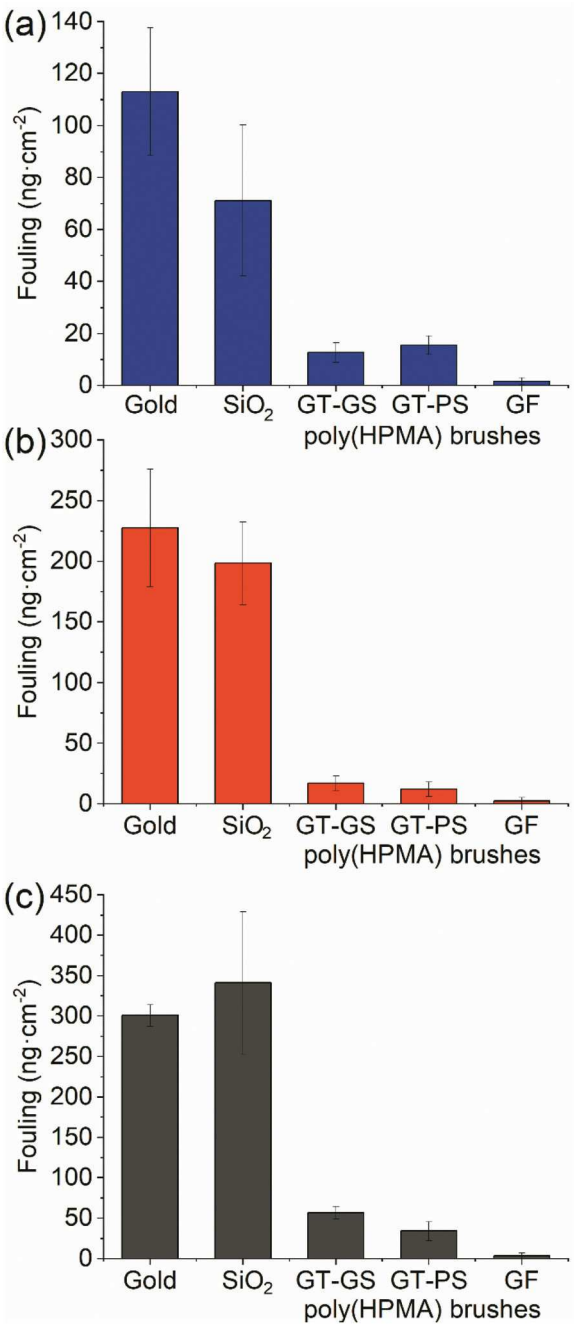

Fig. 4 Non-specific protein adsorption of (a) human serum albumin (HSA, 5 mg mL^{-1}), (b) fibrinogen (Fbg, 1 mg mL^{-1}), and (c) human blood plasma (HBP).

increase in grafting density for the GT-PS-layer probably accounts for its superior antifouling performance against HBP.

Poly(HPMA) brushes prepared by GF in the surface-initiated polymerization approach reduced fouling from both single-protein solutions by 99% with respect to bare gold. In comparison with GT-coatings, the fouling on the brush prepared by GF from HSA and Fbg solutions was 5 and 8 times lower, respectively. This corresponds well to the much higher grafting density of the GF-coating providing a more effective barrier

against fouling, even though the polymer molar mass was comparable. While the chain-end functionality of the GT and GF layers is different, its effect on fouling resistance is expected to be negligible due to the very low concentration of end groups as well as their distribution within the polymer layers.[61] The difference in antifouling performance is even more marked for HBP, where the GF-coating reduced the non-specific adsorption by over 99% with respect to the bare gold (Fig. 4). This fouling resistance is on the level of the best antifouling surfaces described in the literature[8,73,74] and 15 times better than GT-GS and 9 times better than GT-PS, once again highlighting the advantage of the GF method, owing to the higher achievable grafting density (see ESI, Fig. S12†).

The comparison of antifouling properties of the poly(HPMA) brush layers prepared by GT and GF highlights the importance of the grafting method in defining the coating properties. Given the comparable polymer chemical structure and molar mass, the grafting method is shown to be the determining factor in achieving improved antifouling performances. The results indicate that the increased grafting density achieved leads to a markedly superior fouling resistance for the GF-poly(HPMA) brush. On the other hand, the layers afforded by the GT method provide a much lower thickness, which may be desirable for certain applications, and they can be obtained by a very simple method. Adjustment of the thermodynamic quality of the solvent allows tuning of the polymer thickness and physical conformation of the chains as desired, and both are related by the polymer molar mass which is controlled before grafting. GF polymerization enables access to higher grafting densities and thicknesses while being able to control the polymer molar mass. Moreover, by immobilizing a lowered surface density of initiating species (or CTA), it is possible to achieve polymer layers of reduced grafting density. However, GF polymerizations require relatively demanding polymerization conditions such as solvent deoxygenation and working under inert atmosphere. Nevertheless, new developments in oxygen-tolerant polymerization techniques are increasingly bypassing these requirements.[75–79] In combination, the GT and GF methods complement each other to provide a versatile toolbox for the surface functionalization with polymer brushes.

Conclusions

We studied the effect of the grafting-to and grafting-from methods on the surface parameters and fouling properties of poly(HPMA) brushes prepared using solution and surface-initiated RAFT polymerization. These brushes were composed of polymer chains of comparable composition and molar mass, as confirmed by size exclusion chromatography and single-molecule force spectroscopy. While both the types of coatings have been demonstrated to substantially reduce the fouling from blood plasma, the coatings prepared using the grafting-from method enabled much better suppression of fouling than the coatings prepared using the grafting-to method. The superior antifouling performance provided by the grafting-from method was linked with a higher grafting density of the polymer brush. The higher grafting density was accompanied by a markedly lower swelling in water, as a result of the reduced polymer conformational freedom. In summary, the reported results link and compare the GT and GF methods, and show how the choice of the grafting method affects the maximum achievable grafting density and, concomitantly, the resistance to non-specific protein adsorption.

Author contributions

The manuscript was written through contributions of all authors. All authors have given approval to the final version of the manuscript.

Conflicts of interest

The authors declare no competing financial interest.

Acknowledgements

This research was supported by the Czech Science Foundation (Contract No. 20-07313S and 19-02739S). Y. M. W. acknowledges support from the Charles University Grant Agency under project 2600-243-251963. A. d. l. S. P. acknowledges support from the Czech Academy of Sciences under project MSM200502001.

References

1 Y. Wang, J. Wu, D. Zhang, F. Chen, P. Fan, M. Zhong, S. Xiao, Y. Chang, X. Gong, J. Yang and J. Zheng, *J. Mater. Chem. B*, 2019, **7**, 5762–5774.
2 S. Lowe, N. M. O'Brien-Simpson and L. A. Connal, *Polym. Chem.*, 2015, **6**, 198–212.
3 O. Sedlacek, B. D. Monnery and R. Hoogenboom, *Polym. Chem.*, 2019, **10**, 1286–1290.
4 J. G. Wu, J. H. Chen, K. T. Liu and S. C. Luo, *ACS Appl. Mater. Interfaces*, 2019, **11**, 21294–21307.
5 R. E. Holmlin, X. X. Chen, R. G. Chapman, S. Takayama and G. M. Whitesides, *Langmuir*, 2001, **17**, 2841–2850.
6 G. B. Sigal, M. Mrksich and G. M. Whitesides, *J. Am. Chem. Soc.*, 1998, **120**, 3464–3473.
7 K. L. Prime and G. M. Whitesides, *J. Am. Chem. Soc.*, 1993, **115**, 10714–10721.
8 C. Blaszykowski, S. Sheikh and M. Thompson, *Chem. Soc. Rev.*, 2012, **41**, 5599–5612.
9 J. L. Brash, in *Proteins at Interfaces III: State of the Art*, ACS Symp. Ser., 2012, vol. 1120, pp. 277–300.
10 E. van Andel, S. C. Lange, S. P. Pujari, E. J. Tijhaar, M. M. J. Smulders, H. F. J. Savelkoul and H. Zuilhof, *Langmuir*, 2019, **35**, 1181–1191.

11 A. de los Santos Pereira, S. Sheikh, C. Blaszykowski, O. Pop-Georgievski, K. Fedorov, M. Thompson and C. Rodriguez-Emmenegger, *Biomacromolecules*, 2016, **17**, 1179–1185.
12 I. Buzzacchera, M. Vorobii, N. Y. Kostina, A. de los Santos Pereira, T. Riedel, M. Bruns, W. Ogieglo, M. Moller, C. J. Wilson and C. Rodriguez-Emmenegger, *Biomacromolecules*, 2017, **18**, 1983–1992.
13 X. Gao, N. Kucerka, M. P. Nieh, J. Katsaras, S. Zhu, J. L. Brash and H. Sheardown, *Langmuir*, 2009, **25**, 10271–10278.
14 J. Svoboda, O. Sedlacek, T. Riedel, M. Hruby and O. Pop-Georgievski, *Biomacromolecules*, 2019, **20**, 3453–3463.
15 H. Lisalova, E. Brynda, M. Houska, I. Visova, K. Mrkvova, X. C. Song, E. Gedeonova, F. Surman, T. Riedel, O. Pop-Georgievski and J. Homola, *Anal. Chem.*, 2017, **89**, 3524–3531.
16 M. Zamfir, C. Rodriguez-Emmenegger, S. Bauer, L. Barner, A. Rosenhahn and C. Barner-Kowollik, *J. Mater. Chem. B*, 2013, **1**, 6027–6034.
17 W. Zhao, Q. Ye, H. Hu, X. Wang and F. Zhou, *J. Mater. Chem. B*, 2014, **2**, 5352–5357.
18 M. Vorobii, A. de los Santos Pereira, O. Pop-Georgievski, N. Y. Kostina, C. Rodriguez-Emmenegger and V. Percec, *Polym. Chem.*, 2015, **6**, 4210–4220.
19 M. Vorobii, O. Pop-Georgievski, A. D. Pereira, N. Y. Kostina, R. Jezorek, Z. Sedlkova, V. Percec and C. Rodriguez-Emmenegger, *Polym. Chem.*, 2016, **7**, 6934–6945.
20 C. Rodriguez-Emmenegger, S. Janel, A. de los Santos Pereira, M. Bruns and F. Lafont, *Polym. Chem.*, 2015, **6**, 5740–5751.
21 C. F. Wertz and M. M. Santore, *Langmuir*, 2002, **18**, 706–715.
22 M. Kim, S. Schmitt, J. Choi, J. Krutty and P. Gopalan, *Polymer*, 2015, **7**, 1346–1378.
23 Y. Han, J. Cui, J. Jin and W. Jiang, *J. Mater. Chem. B*, 2017, **5**, 8479–8486.
24 G. Emilsson, R. L. Schoch, L. Feuz, F. Hook, R. Y. Lim and A. B. Dahlin, *ACS Appl. Mater. Interfaces*, 2015, **7**, 7505–7515.
25 A. H. Jesmer, V. Huynh and R. G. Wylie, *RSC Adv.*, 2020, **10**, 20302–20312.
26 C. Kang, R. Crockett and N. D. Spencer, *Polym. Chem.*, 2016, **7**, 302–309.
27 L. Michalek, L. Barner and C. Barner-Kowollik, *Adv. Mater.*, 2018, **30**, 1706321.
28 H. Otsuka, Y. Nagasaki and K. Kataoka, *Langmuir*, 2004, **20**, 11285–11287.
29 J. Ji, L. X. Feng, Y. X. Qiu and X. J. Yu, *Polymer*, 2000, **41**, 3713–3718.
30 W. Norde and D. Gage, *Langmuir*, 2004, **20**, 4162–4167.
31 R. Gref, M. Luck, P. Quellec, M. Marchand, E. Dellacherie, S. Harnisch, T. Blunk and R. H. Muller, *Colloids Surf., B*, 2000, **18**, 301–313.
32 D. Liu, J. Guo and J. H. Zhang, *J. Mater. Chem. B*, 2016, **4**, 6134–6142.
33 M. Sun, J. Deng, Z. Tang, J. Wu, D. Li, H. Chen and C. Gao, *Colloids Surf., B*, 2014, **122**, 134–142.
34 Z. Wang, L. Scheres, H. Xia and H. Zuilhof, *Adv. Funct. Mater.*, 2020, **30**, 1908098.
35 P. Kingshott, H. Thissen and H. J. Griesser, *Biomaterials*, 2002, **23**, 2043–2056.
36 O. Pop-Georgievski, S. Popelka, M. Houska, D. Chvostova, V. Proks and F. Rypacek, *Biomacromolecules*, 2011, **12**, 3232–3242.
37 A. de los Santos Pereira, A. Cernescu, J. Svoboda, R. Sivkova, I. Romanenko, B. Bashta, F. Keilmann and O. Pop-Georgievski, *Anal. Chem.*, 2020, **92**, 4716–4720.
38 R. Barbey, L. Lavanant, D. Paripovic, N. Schuwer, C. Sugnaux, S. Tugulu and H. A. Klok, *Chem. Rev.*, 2009, **109**, 5437–5527.
39 S. J. Sofia, V. Premnath and E. W. Merrill, *Macromolecules*, 1998, **31**, 5059–5070.
40 L. Michalek, K. Mundsinger, C. Barner-Kowollik and L. Barner, *Polym. Chem.*, 2019, **10**, 54–59.
41 T. Zhang, Y. Du, J. Kalbacova, R. Schubel, R. D. Rodriguez, T. Chen, D. R. T. Zahn and R. Jordan, *Polym. Chem.*, 2015, **6**, 8176–8183.
42 X. Xu, X. Huang, Y. Chang, Y. Yu, J. Zhao, N. Isahak, J. Teng, R. Qiao, H. Peng, C. X. Zhao, T. P. Davis, C. Fu and A. K. Whittaker, *Biomacromolecules*, 2021, **22**, 330–339.
43 N. Nath, J. Hyun, H. Ma and A. Chilkoti, *Surf. Sci.*, 2004, **570**, 98–110.
44 M. Slowikowska, K. Chajec, A. Michalski, S. Zapotoczny and K. Wolski, *Materials*, 2020, **13**, 5139.
45 C. Hentschel, H. Wagner, J. Smiatek, A. Heuer, H. Fuchs, X. Zhang, A. Studer and L. Chi, *Langmuir*, 2013, **29**, 1850–1856.
46 D. Goodman, J. N. Kizhakkedathu and D. E. Brooks, *Langmuir*, 2004, **20**, 6238–6245.
47 T. Tischer, R. Gralla-Koser, V. Trouillet, L. Barner, C. Barner-Kowollik and C. Lee-Thedieck, *ACS Macro Lett.*, 2016, **5**, 498–503.
48 K. Ulbrich, V. Subr, J. Strohalm, D. Plocova, M. Jelinkova and B. Rihova, *J. Controlled Release*, 2000, **64**, 63–79.
49 Y. Tsujii, M. Ejaz, K. Sato, A. Goto and T. Fukuda, *Macromolecules*, 2001, **34**, 8872–8878.
50 C. Rodriguez-Emmenegger, B. V. Schmidt, Z. Sedlakova, V. Subr, A. B. Alles, E. Brynda and C. Barner-Kowollik, *Macromol. Rapid Commun.*, 2011, **32**, 958–965.
51 O. Pop-Georgievski, N. Neykova, V. Proks, J. Houdkova, E. Ukraintsev, J. Zemek, A. Kromka and F. Rypaček, *Thin Solid Films*, 2013, **543**, 180–186.
52 C. Bouchiat, M. D. Wang, J. F. Allemand, T. Strick, S. M. Block and V. Croquette, *Biophys. J.*, 1999, **76**, 409–413.
53 G. Meleshko, J. Kulhavy, A. Paul, D. J. Willock and J. A. Platts, *RSC Adv.*, 2014, **4**, 7003–7012.
54 J. L. Dalsin, L. J. Lin, S. Tosatti, J. Voros, M. Textor and P. B. Messersmith, *Langmuir*, 2005, **21**, 640–646.
55 W. J. Brittain and S. Minko, *J. Polym. Sci., Part A: Polym. Chem.*, 2007, **45**, 3505–3512.

56 S. Orfanidis, *Electromagnetic Waves & Antennas Toolbox*, **https://www.mathworks.com/matlabcentral/fileexchange/4456-electromagnetic-waves-antennas-toolbox**, MATLAB Central File Exchange, 2004. (Retrieved May 18, 2022).
57 A. R. Kuzmyn, A. T. Nguyen, L. W. Teunissen, H. Zuilhof and J. Baggerman, *Langmuir*, 2020, **36**, 4439–4446.
58 C. Zhao, L. Li, Q. Wang, Q. Yu and J. Zheng, *Langmuir*, 2011, **27**, 4906–4913.
59 A. R. Kuzmyn, A. de los Santos Pereira, O. Pop-Georgievski, M. Bruns, E. Brynda and C. Rodriguez-Emmenegger, *Polym. Chem.*, 2014, **5**, 4124–4131.
60 C. Rodriguez-Emmenegger, E. Brynda, T. Riedel, M. Houska, V. Subr, A. B. Alles, E. Hasan, J. E. Gautrot and W. T. Huck, *Macromol. Rapid Commun.*, 2011, **32**, 952–957.
61 A. Halperin, *Langmuir*, 1999, **15**, 2525–2533.
62 D. Jirak, J. Svoboda, M. Filipova, O. Pop-Georgievski and O. Sedlacek, *Chem. Commun.*, 2021, **57**, 4718–4721.
63 Q. Chen, E. S. Kooij, X. Sui, C. J. Padberg, M. A. Hempenius, P. M. Schon and G. J. Vancso, *Soft Matter*, 2014, **10**, 3134–3142.
64 N. Schuwer and H. A. Klok, *Langmuir*, 2011, **27**, 4789–4796.
65 S. Guo, R. Quintana, M. Cirelli, Z. S. D. Toa, V. Arjunan Vasantha, E. S. Kooij, D. Janczewski and G. J. Vancso, *Langmuir*, 2019, **35**, 8085–8094.
66 I. B. Malham and L. Bureau, *Langmuir*, 2010, **26**, 4762–4768.
67 S. T. Milner, *Science*, 1991, **251**, 905–914.
68 S. T. Milner, T. A. Witten and M. E. Cates, *Macromolecules*, 1988, **21**, 2610–2619.
69 P. G. de Gennes, *Scaling concepts in Polymer Physics*, Cornell University Press Ithaca, New York, 1979.
70 K. H. Lau, T. S. Sileika, S. H. Park, A. M. Sousa, P. Burch, I. Szleifer and P. B. Messersmith, *Adv. Mater. Interfaces*, 2015, **2**, 1400225.
71 M. F. Cuddy, A. R. Poda and L. N. Brantley, *ACS Appl. Mater. Interfaces*, 2013, **5**, 3514–3518.
72 D. Voet, J. G. Voet and C. W. Pratt, *Fundamentals of biochemistry*, John Wiley & Sons, Inc., New York, 2013.
73 A. M. C. Maan, A. H. Hofman, W. M. de Vos and M. Kamperman, *Adv. Funct. Mater.*, 2020, **30**, 2000936.
74 L. X. Yu, Y. Hou, C. Cheng, C. Schlaich, P. L. M. Noeske, Q. Wei and R. Haag, *ACS Appl. Mater. Interfaces*, 2017, **9**, 44281–44292.
75 S. Shanmugam, J. T. Xu and C. Boyer, *Macromolecules*, 2016, **49**, 9345–9357.
76 N. Zaquen, A. M. N. B. P. H. A. Kadir, A. Iasa, N. Corrigan, T. Junkers, P. B. Zetterlund and C. Boyer, *Macromolecules*, 2019, **52**, 1609–1619.
77 K. Kaya, B. Kiskan, B. Kumru, B. V. K. J. Schmidt and Y. Yagci, *Eur. Polym. J.*, 2020, **122**, 109410.
78 A. Layadi, B. Kessel, W. Q. Yan, M. Romio, N. D. Spencer, M. Zenobi-Wong, K. Matyjaszewski and E. M. Benetti, *J. Am. Chem. Soc.*, 2020, **142**, 3158–3164.
79 W. Q. Yan, M. Fantin, N. D. Spencer, K. Matyjaszewski and E. M. Benetti, *ACS Macro Lett.*, 2019, **8**, 865–870.